

RESEARCH PAPER RP1176

*Part of Journal of Research of the National Bureau of Standards, Volume 22,
February 1939*

ELASTIC PROPERTIES OF CAST IRON

By Alexander I. Krynitsky and Charles M. Saeger, Jr.

ABSTRACT

An optical method for measuring the deflection of cast-iron transverse-test bars during loading and up to the breaking strength has been developed. Transverse-strength properties were determined on test bars made from three types of cast iron heated to the maximum temperatures of 1,400°, 1,500°, 1,600°, and 1,700° C. Test bars were vertically cast bottom-poured in green-sand molds at 100°, 150°, 200°, and 250° C above the liquidus temperature. Total, plastic, and elastic deflection; modulus of rupture; modulus of relative elasticity; and total, plastic, and elastic resiliency were determined and the microstructure of the test bars was examined.

CONTENTS

	Page
I. Introduction.....	191
II. Method of measuring deflection.....	192
III. Materials and preparation of test bars.....	193
IV. Testing procedure.....	194
V. Physical properties of test bars.....	195
1. Modulus of rupture.....	195
2. Plastic, elastic, and total deflection.....	196
3. Relative modulus of elasticity.....	198
4. Resiliency.....	199
VI. Effect of maximum heating temperature on composition and structure.....	202
VII. Unusual structural features in cast iron.....	204
VIII. Summary.....	206
IX. References.....	207

I. INTRODUCTION

The term "elastic properties" as used in this discussion connotes those complex properties that determine the behavior of cast iron under load. They may be determined from the results of transverse bending tests.

All of the properties of cast iron are related to and, to a large extent, determined by the structure, which consists of a coherent metallic matrix throughout which particles of graphite are dispersed. The presence of these particles decreases the amount of metallic material available to resist stressing in a given section and causes nonuniform distribution of stresses, but the quantitative interpretation of these effects is as yet unsettled. In the consideration of the behavior of cast iron in compression, the question whether the spaces occupied by the graphite particles should be considered as voids or as spaces filled with compressible, partly compressible, or incompressible material,

has been discussed by several authors, for example, MacKenzie [1],¹ Thum and Ude [2], Meyersberg [2a], Pearce [3], and Bolton [4]. Aside from the general weakening or depreciation of properties, because of the presence of the relatively soft graphite flakes, the nonhomogeneous structure frequently leads to erratic results in determinations of the properties and renders their interpretation uncertain. Such factors as the composition, shape, size, and surface condition of the specimen, and the details of the testing procedure are of greater importance in determining the properties of cast iron than in similar determinations on other metals, steel, for example.

The determination of the elastic properties of cast iron is further complicated by the fact that even moderate stresses produce plastic as well as elastic deformation in this material. Attention was called to this fact approximately 50 years ago, by de Segundo [5] and by Bach [6]. The observations of these early investigators have been confirmed by subsequent workers, and it had been definitely established that plastic deformation of cast iron begins under low loads. In the determination of elastic properties by means of transverse tests it is necessary, therefore, to define complete stress-deflection curves by means of step-wise loading, and to determine for each load not only the total deflection under load but also the plastic deformation or permanent set that remains in the bar after the load has been removed. The difference between the total and the plastic deformation is the elastic deformation.

Interpretation of the results of transverse tests and of the data computed from these results, for example, modulus of elasticity, resilience, et cetera, in terms of properties such as brittleness, toughness, ductility, and energy required to break a bar has been widely discussed but the correlations have not been entirely satisfactory partly because of the difficulties of conducting transverse tests, with resultant uncertainty regarding the accuracy and reliability of the data obtained.

Preliminary results of this investigation, presented in a previous publication [7], showed that various properties, including the transverse strength and running quality during casting as well as the size and distribution of the graphite flakes in each of the irons used, were affected by the maximum temperature to which the liquid metal had been heated. Computations of the modulus of elasticity were made, based on the data obtained under loads of 1,200 pounds and also under the loads that caused rupture. These results clearly showed the need for a more detailed and systematic study of the stress-strain relations in cast iron. For the present investigation, it was decided to prepare test bars from each of several irons, representing different maximum heating and pouring temperatures, and to record, as accurately as possible, the complete stress-strain curves up to the breaking point of each bar, by means of observations of the successive deflections under increasing loads and the permanent set that accompanied the application of each load.

II. METHOD OF MEASURING DEFLECTION

One of the first requirements for the proposed investigation was an improved method of measuring the deflection of the bar under load

¹ Figures in brackets indicate the literature references at the end of this paper.

and the permanent set in the bar after the load was removed. Direct observation of the changing position in space of a reference mark on the bar is unsatisfactory because it involves a number of assumptions, for example, the supports and the testing machine as a whole must remain immovable and there must be no penetration of the supports into the specimen. To avoid these possibilities of error a new method of measuring deflection was devised, as follows:

In this new method of measuring deflection of bars under transverse loading, a rubber band, *B*, is stretched tightly along the length of the bar, *A*, and is held in position by two clamps, *C*, as shown in figure 1. Metal strips on the inner surface of the clamps keep the rubber band near to, but not in contact with the surface of the bar at all times. The spacing between the two clamps is the same as that between the supports for the bar in the testing machine, 18 inches in these experiments. Reference mark *D* is attached directly to the bar, midway between the clamps. The bar is placed in the testing machine and the micrometer telescope, *E*, mounted at a distance of 20 inches from the bar, is used to measure the distance between the lower edge of the rubber band and the top edge of the reference mark. When the bar deflects under load, the reference mark moves away from the rubber band which remains as a straight line connecting the central portions of the bar at the two supports. The distance between the rubber band and the reference mark therefore indicates the deflection of the loaded bar and a similar measurement after the load is removed indicates the permanent set. With this apparatus, the maximum error in reading deflections, including errors in the micrometer telescope and personal errors of the observer, was found to be less than ± 0.002 inch.

The principal advantage of this simple method of measuring deflections is that the readings are made entirely independently of the testing machine and supporting fixtures. A further advantage is that observations can be continued up to and including the breaking load without danger to sensitive optical apparatus or to delicate instruments such as extensometers.

III. MATERIALS AND PREPARATION OF TEST BARS

Three types of iron, of the compositions shown in table 1, were used in this investigation. Iron *A* is a stove-plate pig iron remelted with the addition of 10 percent of open-hearth ingot iron. Iron *B* approximates the composition of a medium cylinder iron, although the carbon is slightly high and the phosphorus is somewhat low. Iron *C* represents a soft iron such as is used for general castings.

TABLE 1.—Composition of stock pig irons

Iron	Total carbon	Silicon	Manganese	Phosphorus	Sulfur
	<i>Percent</i>	<i>Percent</i>	<i>Percent</i>	<i>Percent</i>	<i>Percent</i>
<i>A</i>	3.44	1.40	0.15	0.46	0.020
<i>B</i>	3.79	1.40	.63	.181	.062
<i>C</i>	3.44	2.43	.77	.395	.050

Cylindrical bars for the transverse tests were cast in groups of four, as shown in figure 2. The pattern was molded in a three-part cylindrical flask with the full length of the test bars contained in the cheek. Each flask contained two groups, that is, eight bars. The patterns were molded in a mixture of eight parts of molding sand and one part of sea coal, tempered to approximately 7 percent of moisture. The mold cavities were faced with nongraphitic carbonaceous material² of commercial origin. The castings were bottom poured with the bars occupying vertical positions in the mold. By this procedure, as described in a previous publication [8], test bars can be produced which are satisfactorily uniform in diameter throughout their length and free from burnt-on sand or other surface defects. The cylindrical section of each bar was 21 inches in length and 1.2 inches in diameter.

Charges of 230 pounds of iron, in a commercial magnesia crucible, were melted in a high-frequency induction furnace of the tilting type. Each melt was heated to a predetermined maximum temperature of 1,400°, 1,500°, 1,600°, or 1,700° C and was maintained at this temperature for approximately 1 minute. The metal was then allowed to cool until the temperature was 250° C above the liquidus temperature³ of the iron used in that particular melt. A set of four bars was then cast as a unit by pouring the metal directly from the tilted furnace into the mold. The metal remaining in the crucible was allowed to cool to the next pouring temperature, 200° C above the liquidus, and another set of four bars was cast. By continuing this procedure, a set of four bars was cast at 150° C above the liquidus, and a final set at 100° C above the liquidus. Sixteen test bars, representing four pouring temperatures, could be thus obtained from a 230-pound melt that had been heated to a definite maximum temperature. The bars were allowed to remain in the molds for at least 18 hours after casting.

Temperature measurements of the molten iron up to 1,600° C were made with a platinum-platinum 10-percent rhodium thermocouple that was protected by a closed-end, glazed porcelain tube inserted in a closed-end graphite tube. The portion of the graphite tube that came in contact with the molten iron was protected by a coating of aluminum oxide covered with a mixture of 95 percent of zirconium silicate and 5 percent of bentonite.

Temperatures above 1,600° C were measured with an optical pyrometer which had been previously calibrated with the thermocouple in the temperature range of 1,400 to 1,600° C.

IV. TESTING PROCEDURE

A universal testing machine of the hydraulic type of 50,000 pounds capacity was used for the transverse tests. The rate of loading of all bars corresponded to 0.12 inch per minute travel of the free cross head of the testing machine.

The test bar, equipped with the rubber band and reference mark, as shown in figure 1, was mounted in the testing machine on two supports of the roller type, at a span of 18 inches. The bar was adjusted until the rubber band lay in the horizontal plane of the neutral axis of the bar. A load of 50 pounds was sufficient to seat the bar firmly but was not enough to produce noticeable plastic deflection, was ap-

² Approximate analysis: 4 percent of volatile; 74 percent of fixed carbon; 22 percent of ash.

³ The liquidus temperature of each iron was estimated from its composition, according to the procedure described in a previous publication [7].

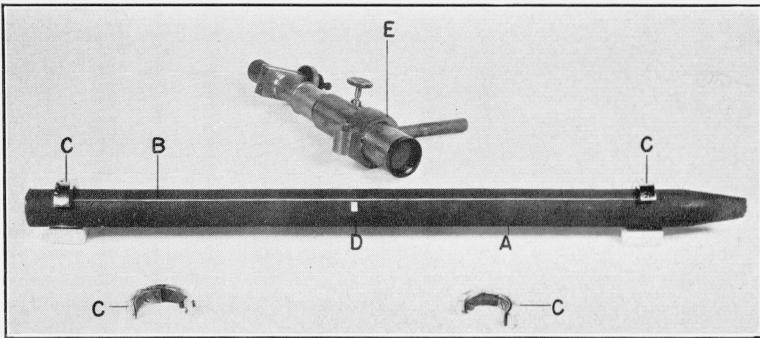


FIGURE 1.—Apparatus for measuring the deflection of test bars under transverse loading.

A, cast-iron test bar; *B*, rubber band; *C*, clamps; *D*, reference mark; and *E*, micrometer telescope.

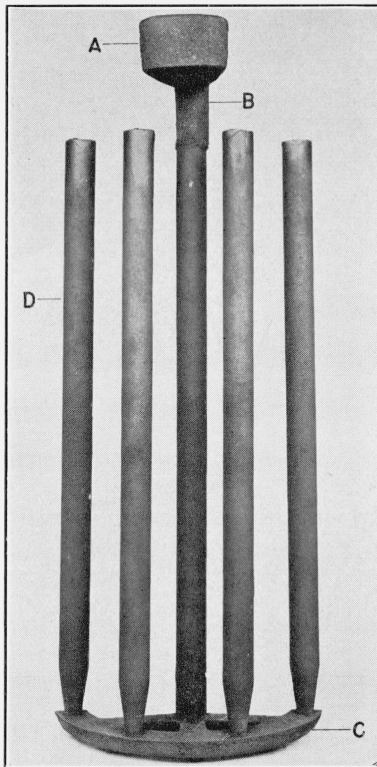


FIGURE 2.—Transverse test bars, as cast.

A, pouring basin; *B*, down gate; *C*, semicircular feeder for bottom pouring; and *D*, vertically cast bars.

plied and the distance between the edge of the rubber band and the top of the reference mark was determined as a zero reading. The bar was then loaded in a series of steps (100 or 200 pounds each) until the breaking load was reached and the deflection of the bar under each of the loads was recorded. After the load reached 800 or 1,000 pounds, each application of a load was followed by unloading to the original 50-pound load, and the permanent set in the unloaded bar was determined. Attempts to record the small permanent deformations that resulted from loads of less than 800 or 1,000 pounds were seldom made. Unloading the bars did not affect the deflection under subsequent loads; the breaking loads and the load-deflection curves of duplicate bars were practically identical when one of the bars was loaded in the manner just described and the other was progressively loaded without unloading between successive loads.

V. PHYSICAL PROPERTIES OF TEST BARS

The results of the transverse tests yielded information on the following properties of the cast iron bars: Modulus of rupture; plastic, elastic, and total deflection; relative modulus of elasticity; and resilience.

1. MODULUS OF RUPTURE

The modulus of rupture of each bar was calculated, according to the formula

$$M = \frac{2.546LS}{D^3},$$

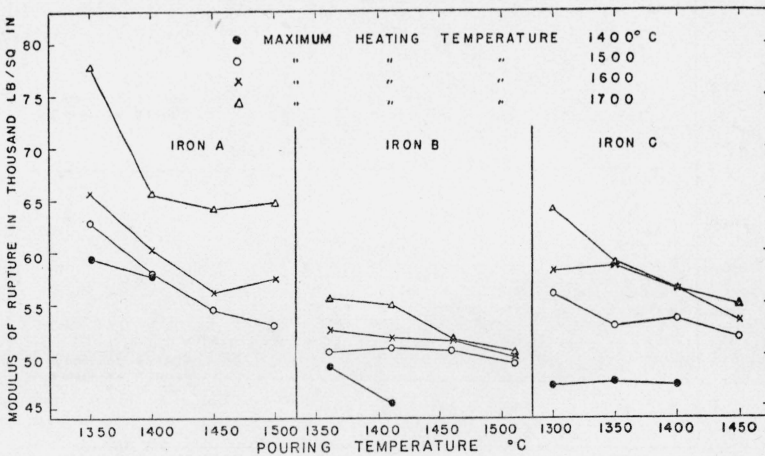


FIGURE 3.—Effect of maximum heating temperature and pouring temperature on the modulus of rupture of three irons.

where M is the modulus for round bars; L , the span of the bar between supports; S , the breaking load; and D , the diameter of the bar.

The modulus of rupture for each of the three irons and the effect on the modulus of varying the maximum heating and pouring temperatures are shown in figure 3. Each of the plotted points is an average of values derived from four companion bars.

The modulus of rupture of iron *A* was found to be considerably higher than that of either of the others; and that of iron *B* to be the lowest of the three. For all of the irons the modulus increased with an increase in the maximum heating temperature and tended to decrease with an increase in pouring temperature, the latter effect being more pronounced for iron *A* than for *B* and *C*.

2. PLASTIC, ELASTIC, AND TOTAL DEFLECTION

The total and plastic deflections or "set" of each bar under increasing loads, were determined and the elastic deflection was taken

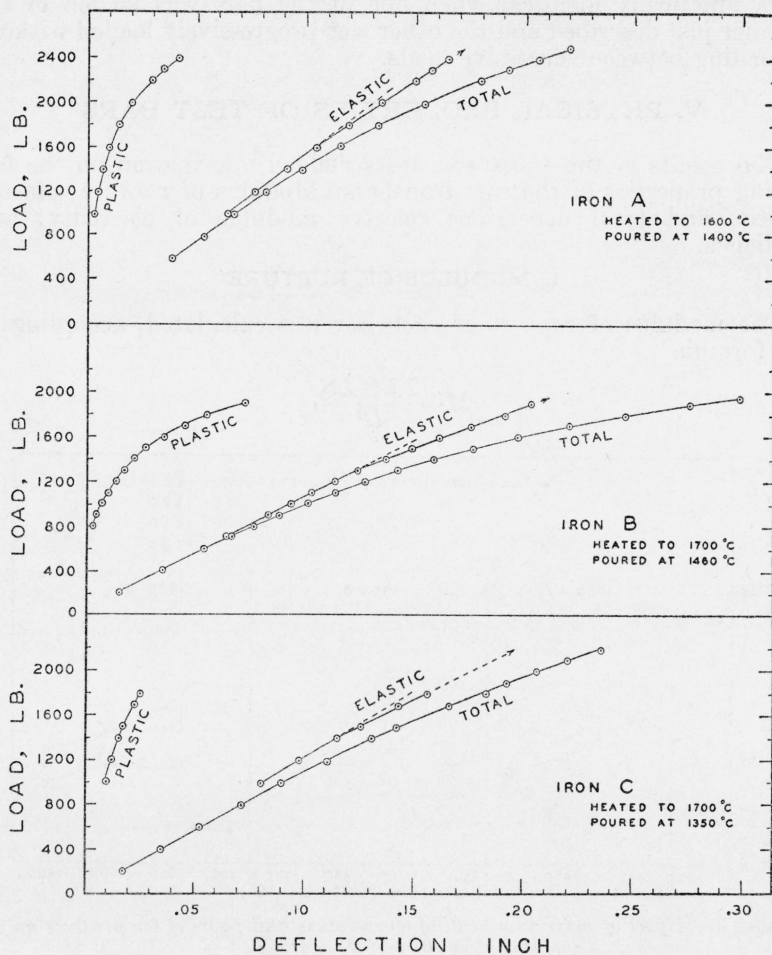


FIGURE 4.—Typical plastic, elastic, and total deflection curves of irons *A*, *B*, and *C*.

as the difference between the total and the plastic deflection for each load.

The relation between load and total, plastic, and elastic deflections of representative bars of irons *A*, *B*, and *C* is shown in figure 4. Iron *A* has the highest breaking strength of the three irons and has about

the same deflection at the breaking load as iron *C*. Iron *B* has about the same breaking load as iron *C* but considerably more deflection at rupture.

In all cases the total deflection curve is a continuous curve inclining progressively towards the deflection axis. If there is any linear portion in the total deflection curve it is confined to the region of very light loads. The curves for plastic deformation for loads of 800 pounds or more, likewise, are continuous curves without straight portions. These observations are in accord with those of previous investigators but the data for elastic deflection are not. Meyersberg [2a] concluded that the upper portions of the elastic elongation curves were slightly bent, whereas Pearce [3] found that the elastic deflection curve usually was a continuous straight line for all loads. The results of this study, illustrated in figure 4, show that the elastic deflection curve is linear only in its lower portion. For iron *A*, the linear portion extends to some load between 1,400 and 1,800 pounds for each of the bars. For irons *B* and *C* it extends to the range of loads from 1,200 to 1,400 pounds. Above the linear portion, each curve inclines toward the deflection axis.

The departure from linearity in these curves can be demonstrated mathematically by the method suggested by Tuckerman in the discussion of a paper by Templin [9]. Theoretical values for the elastic deflection for each load can be calculated from the equation for a straight line and from the modulus of elasticity of the bar at a load within the initial, straight portion of the curve. As long as the curve conforms to the equation for a straight line the observed and calculated values will be in agreement, within the limits of experimental error. Any systematic or appreciable divergence of the observed and calculated values indicates a deviation of the curve from the equation for a straight line.

TABLE 2.—Observed and calculated elastic deflection for iron *B*

Comparison of observed values for elastic deflection with values calculated from the relative modulus of elasticity, 12,445,000 lb/in.², of this bar under a load of 1,000 pounds.

Load	Elastic deflection		
	Observed	Calculated	Difference
<i>Pounds</i>	<i>Inches</i>	<i>Inches</i>	<i>Inches</i>
700	0.064	0.066	-0.002
800	.075	.075	.000
900	.083	.085	-.002
1,000	.094	.094	.000
1,100	.104	.104	.000
1,200	.115	.113	+.002
1,300	.124	.123	+.001
1,400	.137	.132	+.005
1,500	.150	.142	+.008
1,600	.161	.151	+.010
1,700	.176	.160	+.016
1,800	.192	.170	+.022
1,900	.204	.179	+.025

These computations were made for a number of the curves. The data in table 2 show the results obtained from a bar of iron *B* heated to a maximum temperature of 1,700° C and poured at 1,460° C. Loads were applied to this bar in increments of 100 pounds, to define

the curves more closely. It is evident that the observed and calculated values for elastic deflection are in agreement, within the limits of experimental error, ± 0.002 percent, for loads of 1,300 pounds or less, but not for loads in excess of this figure. The elastic deflection curve of this bar, therefore, is a straight line only for loads of 1,300 pounds or less.

3. RELATIVE MODULUS OF ELASTICITY

In this investigation the term "relative modulus of elasticity" is used in place of "modulus of elasticity," because it is well known that cast iron does not follow Hooke's law exactly and the term "modulus of elasticity," as applied to cast iron, generally means the relative stiffness of the iron under the particular conditions of loading.

The relative modulus of elasticity, as determined in the transverse test for a single centrally applied load, is determined by the formula

$$E = \frac{Pl^3}{48ID},$$

where

E = relative modulus of elasticity in pounds per square inch,

P = load in pounds,

l = span in inches,

I = moment of inertia, and

D = deflection (at load P) in inches.

Values for D were taken from the elastic-deflection curves. In view of the fact that the elastic-deflection curve was found to be linear only in the lower portion, two values of the relative modulus of elasticity were computed for each bar; E_1 for the straight portion of the elastic-deflection curve, and E_2 for the second portion of the curve, at the point of rupture.

The data in table 3 show that the values for E_1 are consistently higher than for E_2 . For irons A and B the difference between E_1 and E_2 is generally greater than 1,000,000 lb./in.²; for iron C the difference is usually less than this figure.

Values for the relative modulus of elasticity, E_1 , have been plotted in figure 5 to show the variations with different maximum and pouring temperatures. In general, values of E_1 for iron A are higher than those for either of the other irons and, under some conditions of heating and pouring, the values of E_1 for iron B are higher than those for iron C . A tendency for the values of E_1 to increase with an increase in maximum heating temperature is more evident in irons A and B than in iron C . The data for each iron show a slight and somewhat erratic tendency for the values of E_1 to decrease with increasing temperature of pouring.

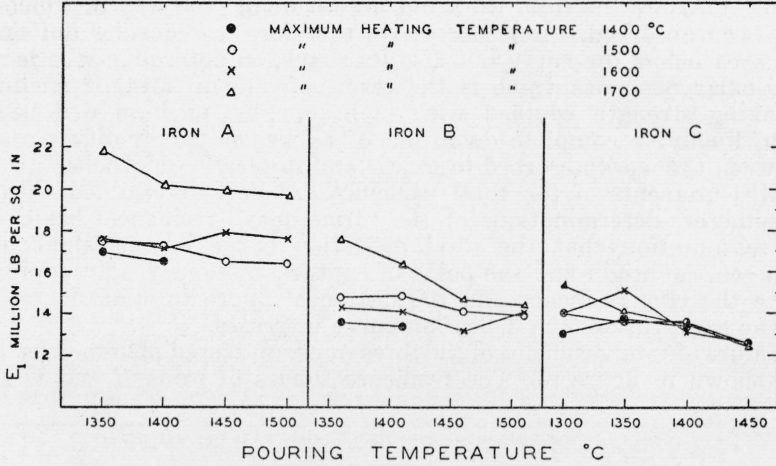


FIGURE 5.—Effect of maximum heating and pouring temperature on the relative modulus of elasticity of cast iron.

TABLE 3.—Relative modulus of elasticity of cast iron

Iron A				Iron B				Iron C			
Temperature		Relative modulus		Temperature		Relative modulus		Temperature		Relative modulus	
Maximum	Pouring	E ₁	E ₂	Maximum	Pouring	E ₁	E ₂	Maximum	Pouring	E ₁	E ₂
°C	°C	Million lb/in. ²	Million lb/in. ²	°C	°C	Million lb/in. ²	Million lb/in. ²	°C	°C	Million lb/in. ²	Million lb/in. ²
1,400	1,400	16.50	15.27	1,410	1,410	13.38	11.92	1,400	1,400	13.37	12.00
1,400	1,350	17.00	15.59	1,410	1,410	13.54	12.15	1,400	1,350	13.71	12.89
1,500	1,500	16.40	15.14	1,510	1,510	13.85	12.51	1,500	1,450	12.58	11.69
1,500	1,450	16.51	15.75	1,510	1,460	14.09	12.63	1,500	1,400	13.57	12.33
1,500	1,400	17.27	16.35	1,510	1,410	14.84	13.47	1,500	1,350	13.58	13.01
1,500	1,350	17.49	15.46	1,510	1,360	14.79	13.08	1,500	1,300	13.97	13.01
1,600	1,500	17.57	16.73	1,600	1,510	14.07	12.30	1,600	1,450	12.55	11.67
1,600	1,450	17.89	17.04	1,600	1,460	13.13	12.40	1,600	1,400	13.17	12.34
1,600	1,400	17.17	16.08	1,600	1,410	14.07	12.80	1,600	1,350	15.10	14.09
1,600	1,350	17.56	16.21	1,600	1,360	14.22	12.95	1,600	1,300	13.97	13.50
1,700	1,500	19.65	18.60	1,700	1,510	14.39	13.01	1,700	1,450	12.42	11.64
1,700	1,450	19.95	18.46	1,700	1,460	14.64	13.17	1,700	1,400	13.48	12.41
1,700	1,400	20.17	18.95	1,700	1,410	16.34	14.47	1,700	1,350	14.10	13.20
1,700	1,350	21.82	19.73	1,700	1,360	17.55	15.63	1,700	1,300	15.36	14.69

* These data are average values of 2 bars. All other figures are averages of 4 bars.

4. RESILIENCE

The resilience of cast iron, the work absorbed by the specimen before rupture, is obtained by measuring the area below the deflection curve and between the origin and an ordinate to the deflection curve at the point of rupture. If the resilience of a specimen could be simply and adequately expressed there would be no need for discussion of "stiffness", "plasticity", "toughness", "brittleness", or similar indefinite but important properties of cast iron. These

values measure the total work but do not define the way in which it has been absorbed. It is necessary, therefore, to consider not only the area below the curve but also its shape, to determine whether a particular resilience value is the result of a high, low, or medium breaking strength coupled with high, low, or medium deflection. And, finally, a complete definition of resilience should differentiate between the work absorbed in elastic and in plastic deformation.

Measurements of the total resilience are best determined with a planimeter; determinations of the "triangular" resilience, based on the assumption that the total deflection curve is a straight line between the origin and the point of rupture, obviously only approximate the true resilience and the degree of approximation decreases as the curvature of the deflection curve increases.

Values of total resilience of the three irons, measured planimetrically, are shown in figure 6. The resilience values of irons *B* and *C* are

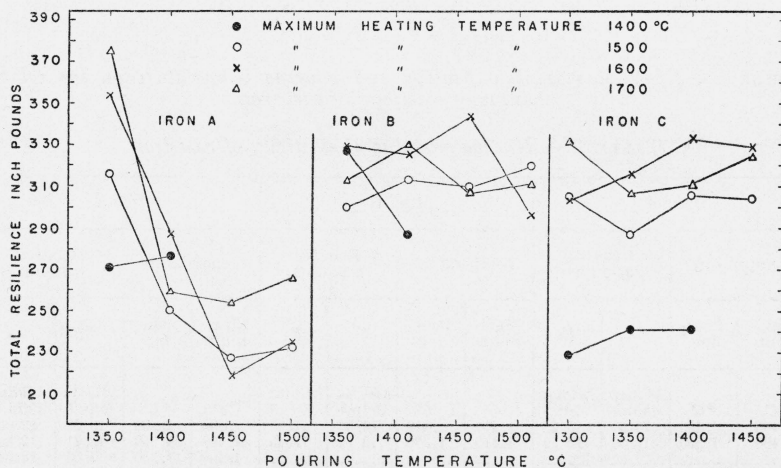


FIGURE 6.—Effect of maximum heating and pouring temperatures on the total resilience of cast iron.

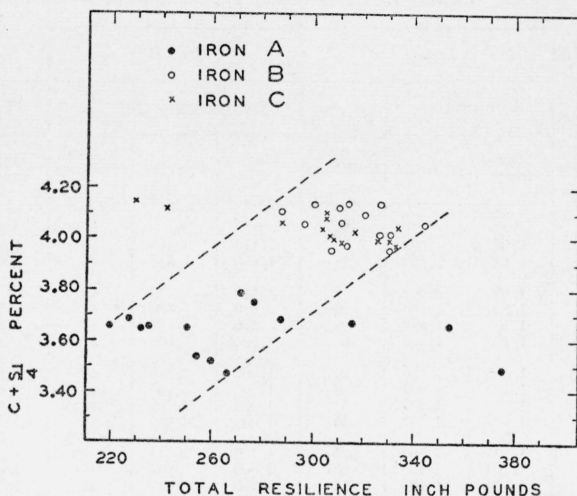
similar. In neither case is there a definite relation to either the maximum heating temperature or the pouring temperature, except that very low resilience values were obtained from iron *C* that had been heated only to 1,400° C. The curves for iron *A* are quite different from those for irons *B* and *C*. For iron *A* there is a pronounced decrease in resilience with increasing pouring temperature, at least up to 1,450° C. An increase in resilience with increasing maximum heating temperature is evident in the bars that were poured at 1,350° C, but this effect is less evident at higher pouring temperatures. Iron *A* under some conditions of melting and pouring showed the highest resilience values of any of the three irons, but under other conditions of melting and pouring its resilience values were lower than any of those of irons *B* and *C*. These resilience values illustrate the marked effect on the characteristics of cast iron of an addition of 10 percent of ingot iron, as in iron *A*.

A number of attempts to establish more satisfactory criteria for evaluating the properties of cast iron have been made in recent years.

MacKenzie [10] found that there was a definite relation between the ratio of the true to the triangular resilience and the ratio of the secant modulus of elasticity at half load to the ultimate modulus of elasticity. These ratios were computed from the data in this investigation, by using values of E_1 for the secant modulus at half load and values of E_2 for the ultimate modulus, but no definite relation between the widely scattered plotted points could be established.

Attempts to correlate resilience values with the carbon and silicon contents also have been made. For example, MacKenzie [1] and Bolton [4] compared resilience values with those representing the carbon content, plus one-fourth of the silicon content. Values of $C+Si/4$, for irons *A*, *B*, and *C* were computed and were plotted against total resilience, as shown in figure 7. The plotted points for each iron are widely scattered, the spread of the resilience values being greater than that of the $C+Si/4$ values. However, there is some indication of an increase in total resilience with increasing values of $C+Si/4$, as is indicated in figure 7 by the two dotted lines that include the majority of the points for all three irons. A similar relation was found for plastic resilience values, but the elastic resilience tended to decrease with increasing values of $C+Si/4$. On the whole, it must be concluded that the relation between resilience and carbon-plus-silicon contents is not definite for these three irons.

FIGURE 7.—Relation of total resilience to carbon and silicon contents.



Tucker [12] concluded that neither the breaking load, deflection, nor resilience values gave reliable indications of the resistance to thermal shock, but that the plastic resilience, expressed in percentage of the total resilience, furnished a measure of the relative toughness of the irons that he investigated. Such values of plastic resilience of the bars in the present investigation were obtained by subtracting from the total resilience the elastic resilience computed on the assumption that the elastic-deflection curve was a straight line between the origin and the breaking point. These values, expressed as percentage of the total resilience, are given in table 4. The data show that the plastic resilience values for each iron are slightly lowered when the maximum heating temperature is 1,600° or 1,700° C; the effect of varying the pouring temperature, after heating to a particular maximum temperature, is not definite.

According to the data in table 4, the ratio of plastic to total resilience (in percent) of iron *B* is definitely higher than that of either of

the other irons, with the values for iron *A* slightly lower than for iron *C*. According to Tucker's data this indicates that the medium cylinder iron *B* is definitely more resistant to thermal shock than either of the other two, and that the soft iron *C* is somewhat better than the high-strength iron *A* in this respect. It is interesting to note the grouping of the three irons classified in this way and according to the total resilience. On the basis of a comparison of the percentage plastic resilience, iron *B* is superior with irons *A* and *C* paired, whereas, if the comparison is based on the total resilience (fig. 6), irons *B* and *C* are quite similar and *A* is different. These results indicate the complexity of resilience determinations and the difficulty of their interpretation.

TABLE 4.—*Relation of plastic to total resilience of three irons*

Iron A			Iron B			Iron C		
Temperature		Ratio of plastic to total resilience	Temperature		Ratio of plastic to total resilience	Temperature		Ratio of plastic to total resilience
Maximum	Pouring		Maximum	Pouring		Maximum	Pouring	
° C	° C	%	° C	° C	%	° C	° C	%
1,400	1,400	32	1,410	1,410	46	1,400	1,400	34
1,400	1,350	28	1,410	1,360	49	1,400	1,350	37
						1,400	1,300	32
1,500	1,500	29	1,510	1,510	48			
1,500	1,450	29	1,510	1,460	46	1,500	1,450	35
1,500	1,400	29	1,510	1,410	47	1,500	1,400	35
1,500	1,350	32	1,510	1,360	45	1,500	1,350	37
						1,500	1,300	35
1,600	1,500	26	1,600	1,510	40			
1,600	1,450	26	1,600	1,460	46	1,600	1,450	35
1,600	1,400	30	1,600	1,410	44	1,600	1,400	33
1,600	1,350	35	1,600	1,360	46	1,600	1,350	33
						1,600	1,300	32
1,700	1,500	27	1,700	1,510	42			
1,700	1,450	26	1,700	1,460	42	1,700	1,450	28
1,700	1,400	26	1,700	1,410	43	1,700	1,400	32
1,700	1,350	30	1,700	1,360	43	1,700	1,350	25
						1,700	1,300	29

• Average value of 2 bars. Other figures are average values from 4 bars.

VI. EFFECT OF MAXIMUM HEATING TEMPERATURE ON COMPOSITION AND STRUCTURE

After completing the transverse tests, the bars were sampled for chemical analysis and for microscopic examination. The analytical data are summarized in table 5, which gives average values, for each iron, for all the metal that was heated to a particular maximum temperature, irrespective of the temperatures at which the bars were poured. Although data on this point are not included in table 5, variations in pouring temperature did not appreciably affect the content of any of the elements determined.

The data show that there was no appreciable variation in the silicon, manganese, phosphorus, and sulfur contents with variations in maximum heating temperature. There was, however, a definite tendency for the total carbon to decrease with increasing temperature of the molten metal. The metal was melted in a magnesia crucible with the surface of the melt exposed to the air. Under these conditions some loss of carbon by oxidation at the higher temperatures

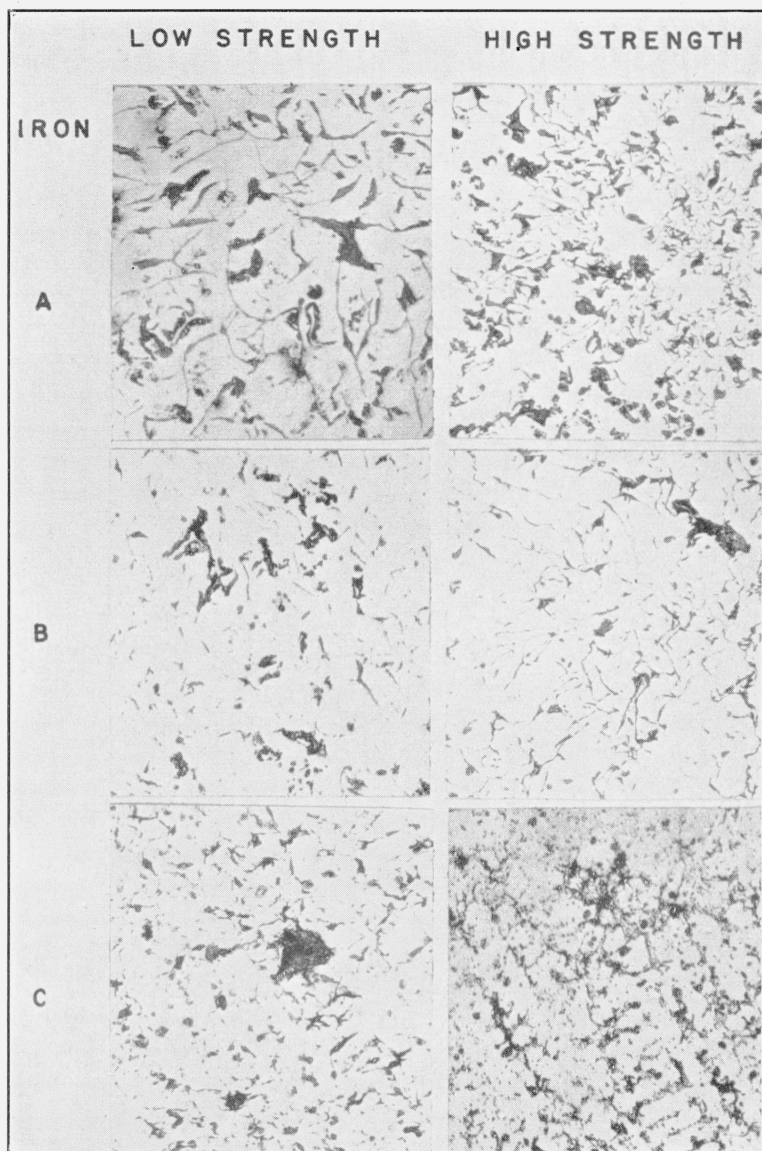


FIGURE 8.—Structure of low- and high-strength bars of irons A, B, and C, unetched;
×100.

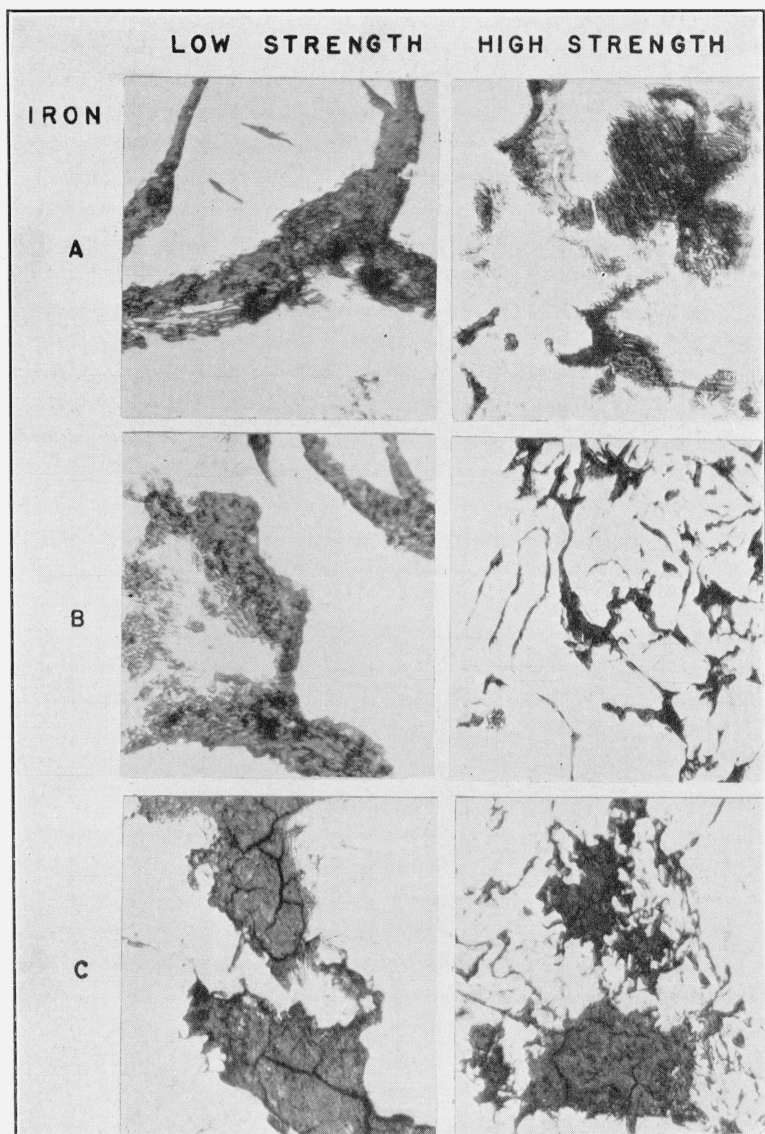


FIGURE 9.—Graphite flakes in low- and high-strength bars of irons A, B, and C, unetched; $\times 500$.

would be expected. The total carbon contents of all the bars are close to or slightly less than the eutectic values computed from the amounts of silicon and phosphorus present. The combined carbon contents of bars of iron *A* are close to the eutectoid composition for the low-strength bars and exceed the eutectoid composition for the high-strength bars. In all bars of irons *B* and *C* the combined carbon is less than the eutectoid amount.

TABLE 5.—Effect of maximum heating temperature on the composition of cast-iron bars

Iron	Maximum heating temperature	Number of bars	Average composition							Breaking load ¹
			Total	Carbon combined	Graphite	Si	Mn	P	S	
	°C		%	%	%	%	%	%	%	lb
<i>A</i> -----	1,400	8	3.46	0.90	2.56	1.24	0.14	0.46	0.024	2,210
<i>A</i> -----	1,700	16	3.20	1.04	2.16	1.22	.15	.46	.025	2,567
<i>B</i> -----	1,410	8	3.82	0.74	3.08	1.25	.48	.172	.059	1,780
<i>B</i> -----	1,700	16	3.66	.72	2.94	1.29	.55	.170	.061	2,010
<i>C</i> -----	1,400	12	3.54	.58	2.96	2.36	.72	.39	.056	1,780
<i>C</i> -----	1,700	16	3.39	.64	2.75	2.38	.75	.40	.058	2,210

¹ Corrected to bar diameter of 1.2 inches.

In general, the strength of cast iron increases with decreasing amounts of graphitic (or total) carbon. Data for the breaking loads, in table 5, show that the bars of iron *A* had higher strengths and lower graphitic carbon contents than the corresponding bars of either *B* or *C*. Furthermore, in each of the three irons, an increase in maximum heating temperature decreased the amount of graphitic carbon and increased the strength. Evidently the strength and associated properties of these irons are affected by the amount of graphitic or total carbon but examination of the microstructure shows that there are variations in the size of the graphite flakes and in their distribution, as well as in the amount of graphitic carbon.

Cross sections of the test bars, from locations close to the fractures, were prepared for microscopic examination, according to the procedure described by Ellinger and Acken [13]. The specimens were ground on a surface grinder, lapped on a lead-tin plate charged with fine emery, further lapped on a second plate charged with finer emery, and, finally polished with an aqueous suspension of rouge, in an automatic polishing machine.

The micrographs in figure 8 show that the high-strength bars of each iron contained smaller and more uniformly distributed particles of graphite than did the low-strength bars of the same iron. The difference in particle size is more readily apparent in the micrographs of representative areas under higher magnification, in figure 9, and the structure of the nongraphitic matrix of each bar, revealed by etching the polished specimen, is shown in figure 10. The latter micrographs show that the matrix of the low-strength bars of iron *A* (heated to 1,400° C) is coarsely pearlitic, whereas in the high-strength bars of the same iron (heated to 1,700° C) large amounts of massive cementite are present, which, by stiffening and hardening the matrix, undoubt-

edly contributed to the high strength of these bars. Cementite is found only in iron that contains hypereutectoid amounts of combined carbon; pearlitic structures are associated with eutectoid and hypoeutectoid compositions. For iron *B*, the matrix of both high- and low-strength bars was found to be pearlitic, with small amounts of ferrite present and the structure of both high- and low-strength bars of iron *C* was found to consist of fine pearlite with areas of ferrite and of steadite.

The relations between the strengths, compositions, and structures of the three irons may be summarized as follows:

1. The increase in strength of each of the irons after it has been heated to a high temperature is associated with a decrease in the amount of graphitic carbon and in the size of the graphite particles and with an increase in the uniformity of their distribution.

2. The high strength of iron *A*, as compared to irons *B* and *C*, is associated with lower graphitic carbon and higher combined carbon contents.

VII. UNUSUAL STRUCTURAL FEATURES IN CAST IRON

An unusual structural condition was observed in many of the graphite flakes of iron *C*, in which an appreciable portion of the graphite appeared to be subdivided into roughly hexagonal grains. This condition is readily apparent in the micrograph of low-strength iron *C*, in figure 9, and is also evident, although less pronounced, in the micrograph of a high-strength iron *C*. Nipper [14] observed similar structures in samples of graphite laminas, but it is not entirely clear from his paper whether these laminas are natural graphite or have been isolated from cast iron. The present example of hexagonal graining in graphite refers definitely to the structure of graphite in cast iron.

Several of the specimens of iron *C* also showed a tendency towards a dendritic structure in the arrangement of graphite particles. This tendency is evident in portions of the micrograph of the high-strength bar of iron *C*, in figure 8, but in no case was the dendritic structure developed to such an extent that the properties of the bar were definitely affected.

Several of the micrographs in figure 9 suggest the existence of a laminated structure in some of the graphite particles. Examination under higher magnification confirmed this suggestion by showing that laminated areas existed in some of the large graphite particles and that the structure of some of the smaller particles was almost entirely laminated, as is shown by the micrographs in figure 11. This condition was most pronounced in specimens from high-strength bars of iron *A*, in which the combined carbon is hypereutectoid, but was also observed in hypoeutectoid, low-strength bars of iron *A* and occasionally in both high- and low-strength bars of iron *B*. These laminated structures were observed in specimens from the unstrained ends of the bars as well as in specimens from locations adjacent to the fractures and, therefore, were not caused by stress deformation of graphite particles during transverse loading. Furthermore, the laminated appearance persisted through repeated repolishings and hence was not an accidental or surface phenomenon.

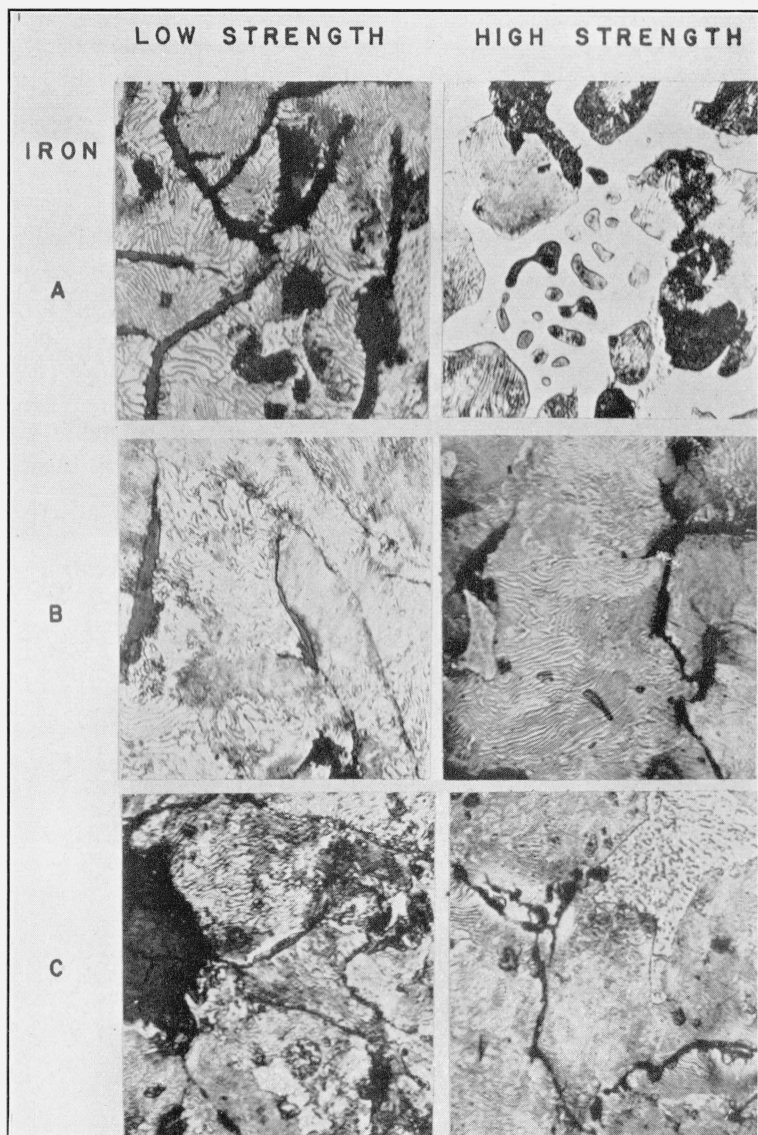


FIGURE 10.—Matrix structure in low- and high-strength bars of irons A, B, and C.
Etched with 1-percent solution of nitric acid in ethyl alcohol; $\times 500$.

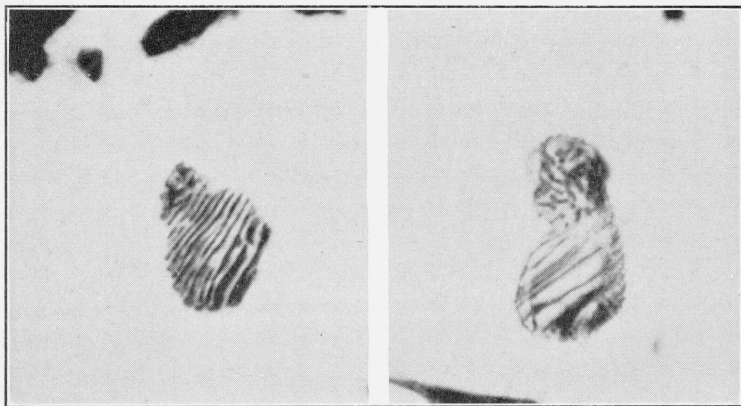


FIGURE 11.—*Laminated structure in small graphite particles, unetched; $\times 2000$.*

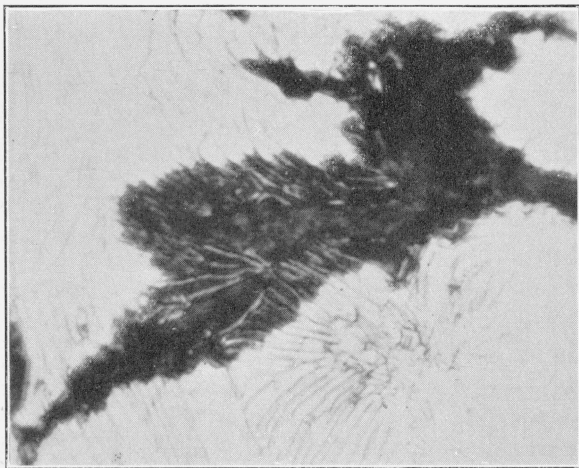


FIGURE 12.—*Eutectoid structure in a flake of graphite.*
Etched with 1-percent solution of nitric acid in ethyl alcohol; $\times 2000$.

Discussion of the mechanism of formation of graphitic particles involves the controversial questions of the double iron-carbon diagram, that is, the question whether graphite in cast iron is formed at eutectic or eutectoid temperatures, or both. Arguments for and against the double diagram were reviewed by Epstein [15], who concluded that the existence of the iron-graphite eutectic had been confirmed by observations of eutectic-like structures and that the existence of the iron-graphite eutectoid had been indicated by the results of thermal analyses, although no one had been able to illustrate satisfactorily the appearance of the iron-graphite eutectoid. In a recent paper Wells [16] concluded that the iron-graphite eutectoid occurs at 738° C and 0.69 percent of carbon, and that the graphitization observed in high-purity alloys of iron and carbon resulted directly from decomposition of austenite as well as from decomposition of cementite. Boyles' recent paper [17] indicates that the large flakes of graphite in cast iron were formed during the solidification at eutectic temperatures and that subsequent decomposition of austenite or carbide at subeutectic temperatures produced finely divided graphite which had little effect on the flake structure.

The authors' conclusion that the laminated graphite structure, illustrated in figure 11, was formed by eutectoid decomposition of austenite or carbide is in agreement with the conclusions of these other investigators. Laminated structures have been observed in some examples of eutectic alloys, but the best-known example of laminated structure is pearlite, which consists of alternate laminations of ferrite and cementite in the proportions of the eutectoid composition. The appearance and structure of the laminated graphite are similar to those of pearlite, and it is reasonable to assume that the laminated graphite also is a result of a eutectoid decomposition, one in which austenite (or carbide) decomposes to form laminated graphite and ferrite. The micrographs in figure 11 therefore are offered as photographic evidence of the existence of the iron-graphite eutectoid.

Etching of specimens that contained laminated graphite revealed further unusual structures. Figure 12 shows the appearance of a flake of graphite and its surrounding areas in one of the high-strength bars of iron A, etched with a 1 percent solution of nitric acid in ethyl alcohol. The graphite flake is surrounded by pearlitic areas the structure of which extends into, and at one point entirely across, the graphite. The appearance suggests that the surface of the pearlitic area has been flowed over the graphite in the polishing operation, but there are objections to this suggested explanation. The flow of metal surfaces during polishing has been established by Beilby and subsequent workers, but it is generally agreed that such a flowed film is "amorphous," that is, structureless, and hence different in properties from those of the parent metal. It is difficult to believe that such a layer could preserve the patterns that are shown in figure 12. Moreover, a reasonable explanation of this structure can be developed if it is assumed that both pearlite and the laminated graphite are produced by the eutectoid decomposition of austenite or carbide. Apparently, in the area shown in figure 12, the same eutectoid decomposition that produced pearlite in the surrounding areas formed the laminated structure in the graphitic area. The fact that some of the laminations are common to both the pearlite and the laminated graphite,

indicates that the two structures were formed under the same conditions. These observations further indicate that the laminated graphite structure shown in figure 11 represents the iron-graphite eutectoid mixture. Furthermore, the suggested mechanism of simultaneous formation of pearlite and laminated graphite in adjacent areas accounts for the observation of the existence of the laminated structure in numerous small areas along the boundaries of large grains of graphite, as in figure 9. The structure of the pearlite is not revealed in these polished but unetched specimens.

Although Bolton [18], in a discussion of a somewhat similar structure, suggested that the black area might not be graphite, the authors believe that the black area in figure 12 is graphite, containing definite indications of a laminated structure closely related to the structure of pearlite. The present data do not indicate whether the laminated graphite is formed by eutectoid decomposition of austenite or of carbide. However, Wells [16] has shown that either of these reactions can produce graphite in high-purity iron-carbon alloys.

VIII. SUMMARY

1. A new method of measuring the deflection of test bars under transverse loading has been developed. Measurements of deflection under interrupted loading can be continued up to the breaking point of the bar and the accuracy of these measurements is entirely independent of the rigidity of the testing machine and the mountings of the bar.

2. The properties of three types of cast iron were determined by measurements under transverse loading. Iron *A* was a stove-plate pig iron to which 10 percent of basic open-hearth ingot iron had been added, iron *B* represented the medium cylinder type of cast iron, and iron *C* was a soft iron of the type used for general castings. The average breaking load of iron *A* was appreciably greater than the breaking load of either irons *B* or *C*, and consequently, the elastic properties of *A* were generally superior to those of *B* or *C*.

3. Variations in the maximum temperature to which the liquid metal was heated affected the composition, structure, and properties of the test bars. An increase in the maximum heating temperature decreased the amounts of total and graphitic carbon, decreased the size and increased the uniformity of distribution of the graphite particles, and in general increased the transverse strength and elastic properties. The properties of iron *A* were more susceptible than those of *B* or *C* to variations in the maximum heating temperature.

4. Variations in the temperatures at which the test bars were poured had less effect than variations in maximum heating temperature on the composition, properties, and structure. However, there was a tendency for some of the properties to decrease with increasing pouring temperature, particularly for iron *A*.

5. The results of the transverse tests indicate that the initial portion of the elastic-deflection curve is a straight line, but at approximately half of the breaking load the curve inclines towards the deflection axis. For all bars of iron *A* the points of inflection occurred at loads between 1,400 and 1,800 pounds, for irons *B* and *C* the limiting value lay between 1,200 and 1,400 pounds. Because of the curvature of the elastic-deflection curves, a value for the relative modulus

of elasticity, computed from the data for any point on the initial linear portion of the curve, is approximately 1,000,000 pounds greater than a similar value computed from the load and deflection at the point of rupture.

6. Two unusual structural conditions were observed, indications of the existence of hexagonal-like grains within some of the graphite particles of iron *C*, and evidence of the existence of a laminated structure, resembling that of pearlite, in many of the graphite particles of irons *A* and *B*, particularly the former. The laminated graphite structure is considered to be that of the iron-graphite eutectoid composition.

Grateful acknowledgment is made to L. D. Jones, C. E. Jackson, and G. W. Wells for assistance in this investigation and to H. L. Whittemore for his counsel.

IX. REFERENCES

- [1] J. T. MacKenzie, *Elastic properties of cast iron*, Proc. Am. Soc. Testing Materials **29**, pt. 2, 94 (1929).
- [2] A. Thum and H. Ude, *Die mechanischen Eigenschaften des Gusseisens*, Z. Ver. deut. Ing. **74**, 257 (1930).
- [2a] G. Meyersberg, *Sur la signification du module d'élasticité de la fonte*, La Fonte, No. 14, 522 (1934).
- [3] J. G. Pearce, *The elasticity, deflection, and resilience of cast iron*, J. Iron Steel Inst. (London) **129**, pt. 1, 331 (1934).
- [4] J. W. Bolton, *Gray Cast Iron* (The Penton Publishing Co., Cleveland, Ohio, 1937).
- [5] E. C. de Segundo, *Experiments on the strain in the outer layers of cast iron and steel beams*, Proc. Inst. Civil Engrs. (London) **98**, 308 (1888-1889).
- [6] C. Bach and R. Baumann, *Elasticität und Festigkeit*, 9th ed. (Julius Springer, Berlin, Germany, 1924).
- [7] C. M. Saeger, Jr., and E. J. Ash, *Properties of gray iron as affected by casting conditions*, J. Research NBS **13**, 573 (1934) RP726; Trans. Am. Foundrymen's Assn. **39**, 449 (1933).
- [8] A. I. Krynitsky and C. M. Saeger, Jr., *An improved method for preparing cast iron transverse test bars*, J. Research NBS **16**, 367 (1936) RP880; Trans. Am. Foundrymen's Assn. **45**, 753 (1937).
- [9] R. L. Templin, *The determination and significance of the proportional limit in the testing of metals*, Proc. Am. Soc. Testing Materials **29**, pt. 2, 523 (1929)
- [9a] *Cast Metals Handbook* (Am. Foundrymen's Assn. p. 88, 1935).
- [10] J. T. MacKenzie, *Report of subcommittee 15 on impact testing*, Proc. Am. Soc. Testing Materials **33**, pt. 1, 87 (1933).
- [11] J. T. MacKenzie, *The influence of phosphorus on iron*, Trans. Am. Foundrymen's Assn. **33**, 445 (1925).
- [12] R. C. Tucker, *Pig iron*, Foundry Trade J. (London) **56**, 347 (1937).
- [13] G. A. Ellinger and J. S. Acken, *A Method of Preparation of Metallographic Specimens*. Am. Soc. Metals, Preprint 22 (1938).
- [14] H. Nipper, *Contribution to the study of graphite formation and structure in cast iron and its influence upon the properties of the cast metal*, Foundry Trade J. (London) **51**, 7 (1934).
- [15] S. Epstein, *The Alloys of Iron and Carbon*, **1** (McGraw-Hill Book Co., Inc., New York, N. Y., 1936).
- [16] C. Wells, *Graphitization in high-purity iron-carbon alloys*, Trans. Am. Soc. Metals **26**, 289 (1938).
- [17] A. Boyles, *The Freezing of Cast Iron*, Metals Tech. **4** (April 1937) Tech. Pub. 809, published by American Institute of Mining and Metallurgical Engineers.
- [18] J. W. Bolton, *Graphitization and inclusions in gray iron*, Trans. Am. Foundrymen's Assn. **45**, 467 (1937).

WASHINGTON, October 21, 1938.